Dielectric or plasmonic Mie object at air–liquid interface: The transferred and the traveling momenta of photon[*]

M R C Mahdy[1,2,†], Hamim Mahmud Rivy[1], Ziaur Rahman Jony[1], Nabila Binte Alam[3], Nabila Masud[1], Golam Dastegir Al Quaderi[4], Ibraheem Muhammad Moosa[5], Chowdhury Mofizur Rahman[6], and M Sohel Rahman[5,‡]

[1] *Department of Electrical & Computer Engineering, North South University, Bashundhara, Dhaka 1229, Bangladesh*
[2] *Pi Labs Bangladesh LTD, ARA Bhaban, 39, Kazi Nazrul Islam Avenue, Kawran Bazar, Dhaka 1215, Bangladesh*
[3] *Department of Computer Science & Engineering, Military Institute of Science and Technology, Dhaka, Bangladesh*
[4] *Department of Physics, University of Dhaka, Dhaka, Bangladesh*
[5] *Department of Computer Science & Engineering, Bangladesh University of Engineering and Technology ECE Building, West Palasi, Dhaka-1205*
[6] *Department of Computer Science & Engineering, United International University, Dhaka, Bangladesh*

Considering the inhomogeneous or heterogeneous background, we have demonstrated that if the background and the half-immersed object are both non-absorbing, the transferred photon momentum to the pulled object can be considered as the one of Minkowski exactly at the interface. In contrast, the presence of loss inside matter, either in the half-immersed object or in the background, causes optical pushing of the object. Our analysis suggests that for half-immersed plasmonic or lossy dielectric, the transferred momentum of photon can mathematically be modeled as the type of Minkowski and also of Abraham. However, according to a final critical analysis, the idea of Abraham momentum transfer has been rejected. Hence, an obvious question arises: whence the Abraham momentum? It is demonstrated that though the transferred momentum to a half-immersed Mie object (lossy or lossless) can better be considered as the Minkowski momentum, Lorentz force analysis suggests that the momentum of a photon traveling through the continuous background, however, can be modeled as the type of Abraham. Finally, as an interesting sidewalk, a machine learning based system has been developed to predict the time-averaged force within a very short time avoiding time-consuming full wave simulation.

1. Introduction

In 1908, physicist Hermann Minkowski proposed that the total momentum of an electromagnetic field inside any matter is equal to $\int \boldsymbol{D} \times \boldsymbol{B} \, \mathrm{d}v$.[1] This suggests that the photon momentum should actually increase and take the value $p = n\hbar k_0$ according to quantum description. Here, n is the refractive index of the medium, k_0 is the wave number of the electromagnetic wave in air, and $\hbar$ is the reduced Planck constant. A year later, the German physicist Max Abraham proposed a different argument that the photon inside a medium would have a lower/decreased momentum that is equal to $\int [(\boldsymbol{E} \times \boldsymbol{H})/c^2] \, \mathrm{d}v$, or according to quantum description, the value of photon momentum $p = \hbar k_0/n$.[2] Nearly 100 years later, there is still no clear answer as to which of these formulae is correct.[3–5] According to Ref. [5], "both the Abraham and Minkowski forms of the momentum density are correct, with the former being the kinetic momentum and the latter, the canonical momentum." Notably, there is no simple experiment that supports the decrease of photon momentum (i.e., Abraham momentum of photon) inside a matter except for a few recent reports.[6–8]

One of the recently popularized ideas in the area of photon momentum transfer or optical force is known as tractor beam.[9–11] A tractor beam is a customized light beam that exerts a counter intuitive negative force on a scatterer,[9–16] pulling it opposite to the propagation direction of light, in contrast to the conventional pushing force. Tractor beam experiments, which involve the material background,[12–14] can also be investigated in details to understand the persistently debated roles of different photon momenta such as those of the Abraham–Minkowski controversy.[3–5,17,18] In this article, we have made an attempt to investigate the Abraham–Minkowski controversy based on the tractor beam like effects.

We have investigated the light momentum transfer and related optical force on a scatterer (both absorbing and non-absorbing) floating on an interface of two or three different media (both absorbing and non-absorbing). Prior to this current work, for the interfacial tractor beam experiment, detailed calculations by ray tracing method and stress tensor equations showed that the pulling force is natural in an air–water scheme due to the linear increase of photon momentum

in the infinitely long water medium.[12,14] Interestingly, non-Minkowski formulations[14] show a pushing force contradicting the experimental observation in Ref. [12]. However, the suggested interpretation in favor of Minkowski photon momentum for the interfacial tractor beam experiment has been questioned in Ref. [19]. Two different recent experiments have supported the observation of Abraham photon momentum for the air–water interface.[6,7] An old experiment has suggested the possible observation of Abraham force density,[20] which is also a partial support to the observation of the associated electromagnetic momentum density $[(\boldsymbol{E} \times \boldsymbol{H})/c^2]$ proposed by Abraham. In addition, some notable theoretical works have suggested in favor of the possible existence of Abraham photon momentum[4,5,21–27] for different other situations. A fully alternative explanation by challenging the observation of Abraham photon momentum (in Ref. [7]) has been discussed recently in Ref. [28] and thus, the possible observation on the decrease of linear momentum (i.e., Abraham momentum of photon) has been questioned in Ref. [28] and even for some other situations in Refs. [28–32]. Notably, the experimental 'possible' observation of Abraham photon momentum[8] had also been seriously challenged in prior literature.[31,32]

Considering the inhomogeneous or heterogeneous background, we have theoretically demonstrated that if the background and the half-immersed object are both non-absorbing, the transferred photon momentum to the object can be considered as the one of Minkowski exactly at the interface in time averaged scenario. Remarkably, we have shown that even if the background's width is only a few nano-meter (extremely small in comparison with the object), the half-immersed object experiences an optical pulling force. Several intuitive thought experiments have also been put forwarded to establish this fact. An extremely small gap between the non-absorbing object and the non-absorbing background can fully nullify the increase of the transferred photon momentum at the interface of the object and the gap, which again supports in favor of our previous proposal (the change of momentum of photon exactly at the object and the touching background). Notably, these proposals have been verified based on both full wave simulations and analytical calculations.

In contrast, the presence of loss inside matter, either in the half-immersed object (i.e., plasmonic or lossy dielectric) or in the background, causes optical pushing of the object. Our analytical analysis suggests that for half-immersed plasmonic or lossy dielectric, the transferred momentum of photon can mathematically be modeled as the type of Minkowski and also of Abraham. However, according to a final critical analysis, we have found that the idea of Abraham momentum transfer of photon may lead to some notable problems and hence, it should better be rejected for the case of half-immersed absorbing object.

As a result, considering our analysis in this article (and also several previous works), it appears that the transferred photon momentum to a half-immersed object (absorbing or non-absorbing) or a fully immersed/embedded object[5] (or even to the free carriers[4] inside an absorbing object) can better be modeled as the one of Minkowski (where Minkowski momentum may arise exactly at the interface of two distinct media). Then a question arises: whence the Abraham momentum?

We have demonstrated that though the transferred momentum to a half-immersed Mie object (either lossy or lossless) can better be considered as the Minkowski momentum, Lorentz force analysis along with our full wave simulation results suggests that the momentum of a photon traveling through a host dielectric (i.e., in a continuous background), however, can be considered as the type of Abraham momentum. Interestingly, this conclusion also supports the previous conclusion drawn in a notable work[4] for the lossy semiconductor.

Finally, a machine learning algorithm has been applied to predict the time averaged force on half-immersed objects spending very short simulation time (instead of time-consuming full wave simulations). Apart from our motivation of getting a quick prediction of the force type without a time-consuming full wave simulation, this artificial intelligence-based investigation may open up a novel research avenue by providing us with yet another useful tool/approach to investigate other problems related to optical force and photon momentum inside a matter.

2. Methods

Throughout this paper, we refer to exterior (interior) or outside (inside) forces as those evaluated outside (inside) the volume of the macroscopic objects. We have done all the full wave electromagnetic simulations using COMSOL MULTI PHYSICS software[33] (and few of them have also been verified using Lumerical FDTD software[34]).

Two of the possible proposed set-ups are illustrated in Figs. 1(a) and 1(b). The source is a simple z-polarized (Fig. 1) plane wave $H = H_0 \, e^{i\beta(x\cos\theta - y\sin\theta)}$ (the varying incident angle θ is with the $-x$ axis), where $H_0 = 1$ A/m and the wavelength is always 632.5 nm. The outside optical force[35,36] is calculated by the integration of time averaged external Minkowski[37–41] stress tensor at $r = a^+$ employing the background fields of the scatterer of radius a as follows [in this article, all time averaged forces have been calculated based on this equation]:

$$\left\langle \boldsymbol{F}_{\text{Total}}^{\text{Out}} \right\rangle = \sum \oint \left\langle \overline{\overline{\boldsymbol{T}}} \right\rangle \cdot \mathrm{d}s,$$

$$\left\langle \overline{\overline{\boldsymbol{T}}}^{\text{out}} \right\rangle = \frac{1}{2} \mathrm{Re}[\boldsymbol{D}_{\text{out}} \boldsymbol{E}_{\text{out}}^* + \boldsymbol{B}_{\text{out}} \boldsymbol{H}_{\text{out}}^*$$

$$-\frac{1}{2}\overline{\overline{I}}(E_{\text{out}}^{*}\cdot D_{\text{out}}+H_{\text{out}}^{*}\cdot B_{\text{out}})]. \qquad (1)$$

Here 'out' represents the exterior total field of the scatterer, E, D, H, and B are the electric field, electric displacement field, magnetic field, and magnetic induction field, respectively, $\langle\ \rangle$ represents the time average, and $\overline{\overline{I}}$ is the unity tensor. In contrast, the internal optical force of Minkowski[37,42] is calculated by the integration of time averaged Minkowski stress tensor at $r=a^{-}$ employing the interior fields of the scatterer of radius a as follows:

$$\langle F_{\text{c}}^{\text{in}}\rangle = \langle F_{\text{Mink.}}^{\text{Bulk}}\rangle(\text{in}) = \oint\langle\overline{\overline{T}}^{\text{in}}\rangle\cdot\mathrm{d}s,$$

$$\langle\overline{\overline{T}}^{\text{in}}\rangle = \frac{1}{2}\,\text{Re}[D_{\text{in}}E_{\text{in}}^{*}+B_{\text{in}}H_{\text{in}}^{*}$$
$$-\frac{1}{2}\overline{\overline{I}}(E_{\text{in}}^{*}\cdot D_{\text{in}}+H_{\text{in}}^{*}\cdot B_{\text{in}})]. \qquad (2)$$

Here 'in' represents the interior field of the scatterer. Notably, the internal optical force of Minkowski represents the total conducting force (due to the interaction of the photon with the free charges inside the absorbing objects) inside an object. For lossless objects, equation (2) always yields zero force inside the objects.[37,42]

3. Results and discussion

In the next few subsections, we will demonstrate three specific interesting facts regarding photon momentum inside matter based on both full-wave simulation and analytical analysis: (a) the change of linear momentum of photon exactly at the interface of two distinct media, (b) the change of photon momentum in presence of loss, and (c) the traveling momentum of photon inside a continuous medium.

3.1. Lossless objects: The role of interface on photon momentum transfer

Though the interfacial tractor beam experiment supports the linear increase of photon momentum (i.e., Minkowski momentum), the following question is still a matter of investigation: inside the matter, does the photon momentum always increases, and even if it increases, does it increase throughout the whole medium or just at the interface? In Ref. [43] it has been argued that the increase of linear photon momentum usually occurs at the interface of two different media due to the reduced impedance mismatch. But no conclusive proof is available regarding this very interesting argument given in Ref. [43]. Based on a few proposed thought experiments, we shall first check this proposal for the interfacial tractor beam set-up. However, it should be noted that although we shall show some strong evidence in favor of such proposal (increase of photon momentum specifically at the interface of two different medium[43]), it does not mean that the traveling momentum of photon decreases inside the continuous material medium. Our main focus in the next section is to judge whether the photon momentum really increases at the interface of two distinct media or not (instead of the long continuous material medium). Based on full wave simulations (both 2D and 3D simulations) in COMSOL Multiphysics (FEM method)[33] and Lumerical FDTD (FDTD method),[34] we have made the following three interesting observations.
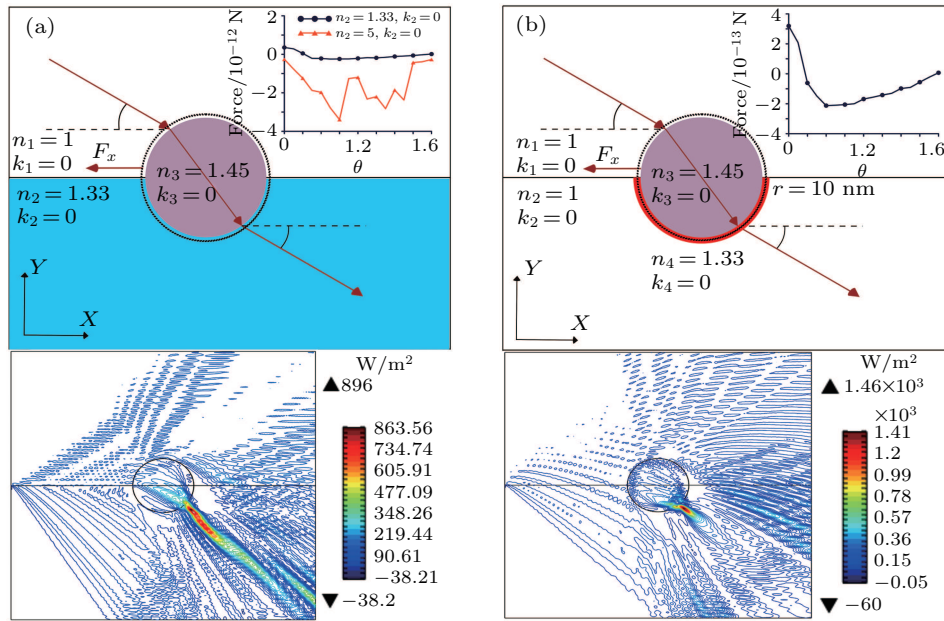

Fig. 1. Diameter of the silica object is 4000 nm and time averaged force has been calculated on the silica object using Eq. (1). The dash line represents the integration boundary. The lower figure shows the Poynting vector distribution for the incident angle of 45° for each specific case. 2D simulation results: (a) object half immersed in air and water medium of index 1.33 (or a medium with refractive index 5). Inset: optical pulling force occurs for different angles of incident light. For the case of index = 5, the optical pulling force increases at least around 100 times than the air–water case for different angles of incident light. Lower figure: Poynting vector distribution for the case where the second background is water. (b) Object half immersed in air and extremely small (width of 10 nm only) background of water. Inset: optical pulling force occurs (almost similar to the force of the air–water case in (a)) for different angles of incident light.

Case 1 From Fig. 1(a), it is evident that if we increase the refractive index of the second medium, the magnitude of the optical pulling force increases, which supports the Minkowski photon momentum. But figure 1(b) reveals that if we consider an extremely small lower background (water) medium (around 10 nm width, where the object diameter is 4000 nm), still a local optical pulling force occurs on the object of 4000 nm. So, the main point is that even for an extremely short touching background, the proposition of the linear momentum increase remains valid. In Fig. 2(a), this fact is again verified with 3D simulations of Fig. 1(b) using short background. To ensure the impact of the short background, we have increased the refractive index of the short background. As expected, the pulling force increases due to the increase of refractive index of the short background as shown in Fig. 2(b). Now, the obvious question arises whether there is any alternative way to verify the robustness of such a proposal. This is addressed next along with few other distinct issues.

Case 2 According to Figs. 1(b), 2(a), and 2(b), the touching short background plays a vital role on the time averaged optical force/transferred momentum of photon under certain specific conditions (i.e., the object should be a Mie object). This fact can also be intuitively guessed simply by putting a silica object such that there would be an extremely small air gap of only 2 nm (i.e., short background width and it is just air) between the lower long background and the object as shown in Figs. 3(a) (2D simulation result) and 3(b) (3D simulation result). Notably, in the 3D case we have used a comparatively larger gap in order to mesh properly.
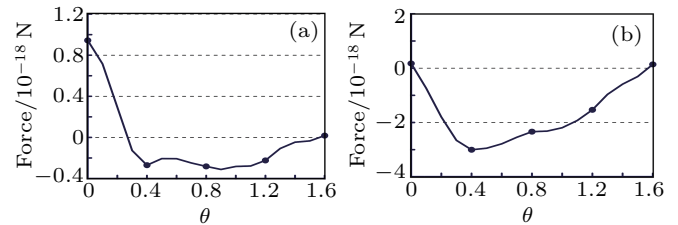

Fig. 2. 3D simulation results: diameter of the silica object is 4000 nm and time averaged force has been calculated on the silica object using Eq. (1). Object half immersed in air and extremely small (width of 10 nm only) touching background of another material. Almost all the parameters are the same as given in Fig. 1(b). Optical pulling force occurs (almost similar to the force of the air–water case in Fig. 1(a)) for different angles of incident light (a) when the short background medium is water, or (b) when the short background medium is a medium of higher refractive index.
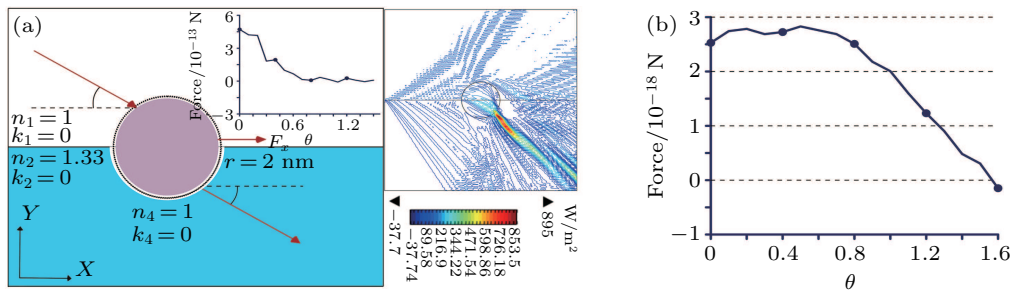

Fig. 3. Diameter of the silica object is 4000 nm and time averaged force has been calculated on the silica object using Eq. (1). The width of the hypothetical short background of air is 2 nm for 2D case and 5 nm for 3D case. The dash line represents the integration boundary. Time averaged optical force is found always pushing when the long background is water (a) for 2D case and (b) for 3D case.

Even if the refractive index of the lower long background is increased up to the value of 1.87 (one of the maximum values of index possible for liquid materials[44]), the force is always found to be a pushing force on the object due to the small gap based on the full wave simulations (both 2D and 3D) shown in Fig. s1 of the supplement material. In contrast, even if the lower long background is air but the short background (width around 10 nm) is just water, the force is found to be a pulling force in Figs. 1(b), 2(a), and 2(b). So, the short background is indeed an imperative criterion, which plays a significant role in such set-ups.

Case 3 Although all the evidences based on full wave simulations (both 2D and 3D) support the linear increase of photon momentum at the interface of two distinct non-absorbing media, there is a notable experimental constraint to verify this interesting proposal of local pulling force of the half-immersed object. For example, it is quite difficult to try to observe the local pulling force of the silica object (only) after putting some water/jelly on the lower body of that silica object. Rather, the movement of the overall object (silica object with water/jelly on its lower body) can be observed much easily in the real-world experiments. Now, the question is whether the whole object (not only Si) meaning Si with water or jelly on its lower body would experience a pulling force or not. The answer is no, the overall object, according to our full wave simulations,[33,34] would experience optical pushing force as shown in Figs. 4(a) (for 2D case) and 4(b) (for 3D case).

But the notable fact is that even this pushing force still supports the initial proposal, i.e., the change of linear momentum of photon exactly at the interface of two distinct non-absorbing media and hence the time averaged pushing or pulling force based on the initial and final momenta of photon for the non-absorbing object. We are explaining this matter analytically in the next sub-section.
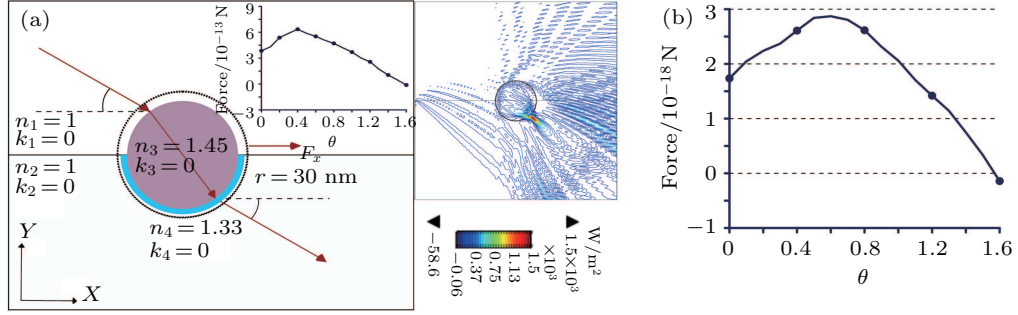
Fig. 4. Diameter of the silica object is 4000 nm and time averaged force has been calculated on the silica object along with the water in the body of the silica object using Eq. (1) (the dash lines are the integration boundary). The width of the hypothetical water layer is 2 nm. Time averaged optical force on the silica object along with the water in the body of the silica object is found always pushing when the long background is air (a) for 2D case and (b) for 3D case.

3.2. Explanation of the observed results for lossless objects: Force due to the initial and final momenta of photon

3.2.1. Based on time averaged optical force laws

One well accepted theory to explain the time averaged total force on any immersed object is the theory of Minkowski on optical force and photon momentum. It is well known that Minkowski stress tensor[27–31,35–37] has a divergence free nature, which suggests that, if the Minkowski stress tensor is applied inside a non-absorbing object employing the internal field of the embedded object, it would lead to zero time-averaged total force. The connection between Eqs. (1) and (2) can be written as

$$\int \left\langle \bar{\bar{T}}_{\text{Mink.}}(\text{out}) \right\rangle \cdot \mathrm{d}s$$
$$= \left\langle F^{\text{total}} \right\rangle = \left\langle F^{\text{Bulk}}_{\text{Mink.}} \right\rangle(\text{in}) + \left\langle F^{\text{Surface}}_{\text{Mink.}} \right\rangle, \quad (3)$$

$$\left\langle F^{\text{Bulk}}_{\text{Mink.}} \right\rangle(\text{in})$$
$$= \left\langle F^{\text{in}}_{\text{c}} \right\rangle = \int \left\langle f_{\text{c}} \right\rangle \mathrm{d}v = \int \frac{1}{2}\text{Re}[(\omega \varepsilon_{\text{I}} E_{\text{in}} \times B^*_{\text{in}})$$
$$- (\omega \mu_{\text{I}} H_{\text{in}} \times D^*_{\text{in}})]\mathrm{d}v, \quad (4)$$

where $\left\langle F^{\text{Surface}}_{\text{Mink.}} \right\rangle$ is known as the time averaged surface force of Minkowski force law which (density of force) is well-known as Helmholtz's surface force density:[45]

$$f^{\text{Surface}}_{\text{Helmholtz}} = \left[-\frac{1}{2} E^2 \Delta \varepsilon - \frac{1}{2} H^2 \Delta \mu \right]_{r=a}. \quad (5)$$

According to Eq. (4), on the boundary (at $r = a$) of any object, the quantity $[\bar{\bar{T}}(\text{out}) - \bar{\bar{T}}(\text{in})] \cdot \hat{n} = f^{\text{Surface}}_{\text{I}}$ ($\hat{n}$ being the local unit outward normal of the object surface) should be exactly the surface force density of Eq. (5). This is calculated next.

From the non-diagonal (ND) components of the Minkowski stress tensors given in Eq. (1) and (2), we obtain

$$[\bar{\bar{T}}^{\text{MIX}}_{\text{Mink}}(\text{out}) - \bar{\bar{T}}^{\text{MIX}}_{\text{Mink}}(\text{in})] \cdot \hat{n}_{r=a}$$
$$= \left\{ [\epsilon_{\text{b}} E^{\perp}_{\text{out}} \cdot E^{\perp}_{\text{out}} - \epsilon_{\text{s}} E^{\perp}_{\text{in}} \cdot E^{\perp}_{\text{in}}] \hat{n} \right.$$
$$+ [\epsilon_{\text{b}} E^{\parallel}_{m\,\text{out}} \cdot E^{\perp}_{m\,\text{out}} - \epsilon_{\text{s}} E^{\parallel}_{m\,\text{in}} \cdot E^{\perp}_{m\,\text{in}}] \hat{m}$$
$$\left. + [\epsilon_{\text{b}} E^{\parallel}_{q\,\text{out}} \cdot E^{\perp}_{q\,\text{out}} - \epsilon_{\text{s}} E^{\parallel}_{q\,\text{in}} \cdot E^{\perp}_{q\,\text{in}}] \hat{q} \right\}_{r=a}$$

$$+ \left\{ [\mu_{\text{b}} H^{\perp}_{\text{out}} \cdot H^{\perp}_{\text{out}} - \mu_{\text{s}} H^{\perp}_{\text{in}} \cdot H^{\perp}_{\text{in}}] \hat{n} \right.$$
$$+ [\mu_{\text{b}} H^{\parallel}_{m\,\text{out}} \cdot H^{\perp}_{m\,\text{out}} - \mu_{\text{s}} H^{\parallel}_{m\,\text{in}} \cdot H^{\perp}_{m\,\text{in}}] \hat{m}$$
$$\left. + [\mu_{\text{b}} H^{\parallel}_{q\,\text{out}} \cdot H^{\perp}_{q\,\text{out}} - \mu_{\text{s}} H^{\parallel}_{q\,\text{in}} \cdot H^{\perp}_{q\,\text{in}}] \hat{q} \right\}_{r=a}. \quad (6)$$

Here, 'MIX' represents the mixed diagonal and non-diagonal elements of the stress tensor, which are not connected with the identity tensor. ε_{b} and μ_{b} are fixed background permittivity and permeability, ε_{s} and μ_{s} are fixed permittivity and permeability of the scatterer. The 'out' represents the total fields (incident plus scattered field) outside a scatterer, 'in' represents the fields inside a scatterer. The electric field at the object and background boundary is defined as $E = E^{\perp}_n \hat{n} + E''_m \hat{m} + E''_q \hat{q}$, where $\hat{n}$, $\hat{m}$, and $\hat{q}$ are the mutually orthogonal arbitrary unit vectors, which are applicable for different co-ordinate systems such as cartesian, spherical or cylindrical. $\hat{n}$ is the local unit normal of the object surface, which is considered aligned towards the direction of wave vector direction (for simplicity). $E^{\parallel}$ and $E^{\perp}$ are the parallel and perpendicular components of electric fields at the background and object boundary. In a very similar way, the magnetic field has also been defined. Now, by employing the electromagnetic boundary conditions in above Eq. (6), we obtain

$$[\bar{\bar{T}}^{\text{MIX}}_{\text{Mink}}(\text{out}) - \bar{\bar{T}}^{\text{MIX}}_{\text{Mink}}(\text{in})] \cdot \hat{n}_{r=a}$$
$$= [\epsilon_{\text{b}} E^{\perp}_{\text{out}} \cdot E^{\perp}_{\text{out}} - \epsilon_{\text{s}} E^{\perp}_{\text{in}} \cdot E^{\perp}_{\text{in}}] \hat{n}_{r=a}$$
$$+ [\mu_{\text{b}} H^{\perp}_{\text{out}} \cdot H^{\perp}_{\text{out}} - \mu_{\text{s}} H^{\perp}_{\text{in}} \cdot H^{\perp}_{\text{in}}] \hat{n}_{r=a}. \quad (7)$$

In contrast, from the pure diagonal (D) components, we obtain (after employing the electromagnetic boundary conditions)

$$[\bar{\bar{T}}^{\text{D}}_{\text{Mink}}(\text{out}) - \bar{\bar{T}}^{\text{D}}_{\text{Mink}}(\text{in})] \cdot \hat{n}_{r=a}$$
$$= -\frac{1}{2} \left\{ [\epsilon_{\text{b}} E^{\perp}_{\text{out}} \cdot E^{\perp}_{\text{out}} - \epsilon_{\text{s}} E^{\perp}_{\text{in}} \cdot E^{\perp}_{\text{in}}] \hat{n} \right.$$
$$+ [\varepsilon_{\text{b}} E^{\parallel}_{m\,\text{out}} \cdot E^{\parallel}_{m\,\text{out}} - \varepsilon_{\text{s}} E^{\parallel}_{m\,\text{in}} \cdot E^{\parallel}_{m\,\text{in}}] \hat{m}$$
$$\left. + [\varepsilon_{\text{b}} E^{\parallel}_{q\,\text{out}} \cdot E^{\parallel}_{q\,\text{out}} - \varepsilon_{\text{s}} E^{\parallel}_{q\,\text{in}} \cdot E^{\parallel}_{q\,\text{in}}] \hat{q} \right\}_{r=a}$$
$$- \frac{1}{2} \left\{ [\mu_{\text{b}} H^{\perp}_{\text{out}} \cdot H^{\perp}_{\text{out}} - \mu_{\text{s}} H^{\perp}_{\text{in}} \cdot H^{\perp}_{\text{in}}] \hat{n} \right.$$
$$+ [\mu_{\text{b}} H^{\parallel}_{m\,\text{out}} \cdot H^{\parallel}_{m\,\text{out}} - \mu_{\text{s}} H^{\parallel}_{m\,\text{in}} \cdot H^{\parallel}_{m\,\text{in}}] \hat{m}$$
$$\left. + [\mu_{\text{b}} H^{\parallel}_{q\,\text{out}} \cdot H^{\parallel}_{q\,\text{out}} - \mu_{\text{s}} H^{\parallel}_{q\,\text{in}} \cdot H^{\parallel}_{q\,\text{in}}] \hat{q} \right\}_{r=a}. \quad (8)$$

Now, by adding Eqs. (7) and (8) and after doing some calculations, we get exactly the surface force law of Helmholtz at the object boundary (Eq. (5) stated previously)

$$f_{\text{Helmholtz}}^{\text{Surface}} = \left[-\frac{1}{2} E^2 \Delta\varepsilon - \frac{1}{2} H^2 \Delta\mu \right]_{r=a}.$$

After doing aforementioned detail analytical calculations, we have shown that we get exactly Eq. (5), the surface force law of Helmholtz, at the object boundary from the quantity $[\bar{\bar{T}}(\text{out}) - \bar{\bar{T}}(\text{in})] \cdot \hat{n} = f_1^{\text{Surface}}$.

So, the difference between the internal Minkowski stress tensor and the external Minkowski stress tensor, exactly at the object and background interface, leads to the Helmholtz's surface force. The time averaged pulling force observed in the interfacial tractor beam experiment can be explained/calculated solely based on this Helmholtz's surface force given in Eq. (5) [which appears just at the interface of two different media (also for different other situations, see Figs. 10(a), 10(b), and 12(a) given in Ref. [45])] and the linear increase (or the transfer) of the photon momentum occurs exactly at the interface of two different media [Helmholtz/Minkowski force also suggests so]. For example, this last statement can also be written directly based on the analytical equation involving just the initial (entering momentum just at the 1st interface of the object) and final (leaving momentum just at the last interface of the object) momenta of photon as shown in Ref. [45].

One may point a fact that the Helmholtz surface force density also arises exactly at the interface of two distinct media for another well-known force density: the Abraham force density[17,20,25] (but not for other well-known force densities like Einstein–Laub force density[25] and Chu force density[25]). But the main focus of this article is to figure out the appropriate momentum of photon associated with the distinct theories of Abraham and Minkowski (or any other theory), instead of figuring out the correctness of Abraham and Minkowski (or any other) stress tensors or force densities. It is important to note that the electromagnetic momentum density of Abraham (and hence the Abraham momentum of photon) is also associated with two other optical force density formulations:[25] the Einstein–Laub force density and the Chu force density. In the next section and later sections, we shall demonstrate that at least for time averaged scenario, the appropriate version of the transferred momentum of photon appears as the one of Minkowski (exactly at the interface or surface regions) instead of the one proposed by Abraham. The above calculations in favor of Helmholtz surface force (which does not appear in Einstein–Laub or Chu force formulations[25]) are nothing but an additional support in favor of the force calculated (at the surface regions) by the corpuscular momentum of photon[45] in the next section (which will support the Minkowski momentum of photon instead of the one of Abraham).

We are now going to apply the idea of initial and final momenta of photon[45] for a simplified case to support our previous three observations by considering a slab object for which the first half is immersed in air but the second/lower half is immersed in water or a material medium.

3.2.2. Based on corpuscular momentum of photon

Let us consider a lossless magneto-dielectric slab of sides at $z = 0$ and $z = d$, embedded (fully immersed) in a magneto-dielectric medium, illuminated at normal incidence by a linearly polarized plane wave propagating along the z direction with time harmonic dependence $e^{i(kz-\omega t)}$. There is an interesting alternative way to calculate the time averaged force known as Lorentz force[46–48]

$$\langle f_{\text{Bulk}(j)} \rangle = \frac{1}{2}\text{Re}[\varepsilon_0(\nabla \cdot E_{\text{in}(j)})E_{\text{in}(j)}^* + \mu_0(\nabla \cdot H_{(j)})H_{\text{in}(j)}^*]$$
$$- \frac{1}{2}\text{Re}[i\omega(\varepsilon_{s(j)} - \varepsilon_b)\{E_{\text{in}(j)} \times B_{\text{in}(j)}^*\}$$
$$+ i\omega(\mu_{s(j)} - \mu_b)\{D_{\text{in}(j)}^* \times H_{\text{in}(j)}\}]. \quad (9)$$

The time-averaged force obtained from fields inside the slab via Lorentz force after a long analytic calculation

$$\left\langle F_{\text{Total}}^{\text{Embedded}}(\text{in}) \right\rangle$$
$$= \frac{1}{2} \frac{E_0^2}{\mu_s\left(\frac{\mu_b\varepsilon_s}{\mu_s\varepsilon_b} - 1\right)} [(\varepsilon_s - \varepsilon_b)\mu_s - (\mu_s - \mu_b)\varepsilon_s]$$
$$\times \{1 + |R|^2 - |T|^2\}, \quad (10)$$

where $\left\langle F_{\text{Total}}^{\text{Embedded}}(\text{in}) \right\rangle$ is the force in per unit area,

$$|R|^2 = \frac{\left(\frac{\mu_b\varepsilon_s}{\mu_s\varepsilon_b} - 1\right)^2 [\sin(k_s d)]^2}{4(\frac{\mu_b\varepsilon_s}{\mu_s\varepsilon_b})[\cos(k_s d)]^2 + \left(1 + \frac{\mu_b\varepsilon_s}{\mu_s\varepsilon_b}\right)^2 [\sin(k_s d)]^2},$$

$$E_x = \begin{cases} \left(e^{jk_b z} + R \cdot e^{-jk_b z}\right)E_0, & z > 0, \\ \left(a e^{jk_s z} + b e^{-jk_s z}\right)E_0, & 0 < z < d, \\ T \cdot e^{jk_b z}E_0, & z < d, \end{cases}$$

$$|T|^2 + |R|^2 = 1, \quad (11)$$

R and T denote the reflection and transmission coefficients of the slab, while a and b are constants determined from the boundary conditions.

An important issue is to verify the agreement of the total Lorentz force with the external Minkowski ST. To simplify, let us consider $\mu_s = \mu_b = \mu_0$ in the above calculations. In Ref. [49] based on the Minkowski ST approach, it has been shown that the total time-averaged external force for a lossless slab is $\left\langle F_{\text{Total}}^{\text{Embedded}}(\text{out}) \right\rangle = \frac{1}{2}\varepsilon_b E_0^2(1 + |R^2| - |T^2|)$, which exactly matches with time-averaged Lorentz force result. However, this force can also be calculated by using a direct approach based on the external photon momentum. For example, we can consider a beam normally incident on the dielectric slab embedded in another dielectric. It has a photon flux $N_i = \langle S \rangle / \hbar\omega$, where the time-averaged Poynting vector is $\langle S \rangle = \frac{1}{2}\sqrt{\varepsilon_b/\mu_0}|E^2|$, being the incident momentum

flux[45] $\tau_i = N_i \hbar k_i$. The reflected beam will have a momentum $\tau_r = N_r \hbar k_r$, where $N_r = |R^2| N_i$. The transmitted (emitted) beam with N_t photons has a momentum flux $\tau_t = N_t \hbar k_t$, where $N_t = |T^2| N_i$. The total force per unit area applied to the dielectric then is

$$\langle \boldsymbol{F}_{\text{Total}}^{\text{Embedded}}(\text{out}) \rangle = \tau_i + \tau_r - \tau_t = N_i \hbar k_i + N_r \hbar k_r - N_t \hbar k_t. \quad (12)$$

Hence, using N_i, the result exactly matches with the time averaged force calculated by both the Lorentz force and Minkowski ST methods.

This last equation is the fundamental equation of the interfacial tractor beam (ITB)[12,14] concept. If the background of the input (light) interface of the slab is air and that of the output interface is water, then only within the Minkowski's approach one will have

$$\tau_t > \tau_i + \tau_r, \quad (13)$$

which according to Eq. (12) will cause an optical pulling on the slab. The interfacial tractor beam experiment supports this fact.[12,14] For a simple bi-background case like that in Refs. [12] and [14], the $|T|^2$ value for the bi-background can be lower than that for the single air background. Hence the only way to consider the pulling effect is attributing $\boldsymbol{p}_{\text{Mink}}(\text{out})$ in Eq. (12) [instead of $\boldsymbol{p}_{\text{Abr}}(\text{out})$] for the momentum transfer from the background. This has also been verified by a full wave simulation for a slab in Figs. 5(a) and 5(c). So, this simple aforementioned approach can explain the linear increase of momentum of photon (due to the reduced impedance mismatch[43]) as shown in Figs. 1(b), 2(a), and 2(b) where an extremely short background has been introduced.

Based on this same approach, it can also be shown that if the rectangular slab (of length d) is fully placed in air just above the water medium (an extremely small/short air layer

between the slab interface and the water interface), the time averaged force will be found positive instead of negative. Such an analysis will also explain the results given in Figs. 3(a) and 3(b): the case of short air background and the pushing force. Interestingly, such a situation (a dielectric slab is placed just in front of a long material background maintaining extremely small gap between them) has already been calculated in Ref. [45] as

$$E_x = \begin{cases} \left(e^{jk_1 z} + R \cdot e^{-jk_1 z} \right) E_0, & z > 0, \\ \left(a e^{jk_2 z} + b e^{-jk_2 z} \right) E_0, & 0 < z < d, \\ \left(c e^{jk_3 z} + d e^{-jk_3 z} \right) E_0, & d < z < W + d, \\ T \cdot e^{jk_4 z} E_0, & W + d < z, \end{cases} \quad (14)$$

$$\langle \boldsymbol{F}_{\text{Total}}^{\text{Embedded}}(\text{out}) \rangle$$
$$= \tau_i + \tau_r - \tau_t = N_i \hbar k_i + N_r \hbar k_r - (N_c + N_d) \hbar k_3, \quad (15)$$

$$\langle \boldsymbol{F}_{\text{Total}}^{\text{Embedded}} \rangle$$
$$= \frac{1}{2} \varepsilon_0 E_0^2 \left(1 + |R|^2 - (|c|^2 + |d|^2) \right). \quad (16)$$

Here usually,

$$(1 + |R|^2) > (|c|^2 + |d|^2). \quad (17)$$

Equation (17) clearly suggests why the time averaged force on the slab should be the pushing one and this has been verified by full wave simulation in Fig. 5(b) [also see Figs. 3(a) and 3(b) for our spherical object set-ups]. Lastly, we can compare (analogy) the case given in Figs. 4(a) and 4(b) with a slightly heterogeneous slab fully immersed in air. Based on the similar analytical approaches as stated above, it indeed leads to the result $\langle \boldsymbol{F}_{\text{Total}}^{\text{Embedded}}(\text{out}) \rangle = \tau_i + \tau_r - \tau_t$ and $(\tau_i + \tau_r) > \tau_t$, supporting a pushing force to the overall object. This has been verified by full wave simulation for a slab in Fig. 5(d).
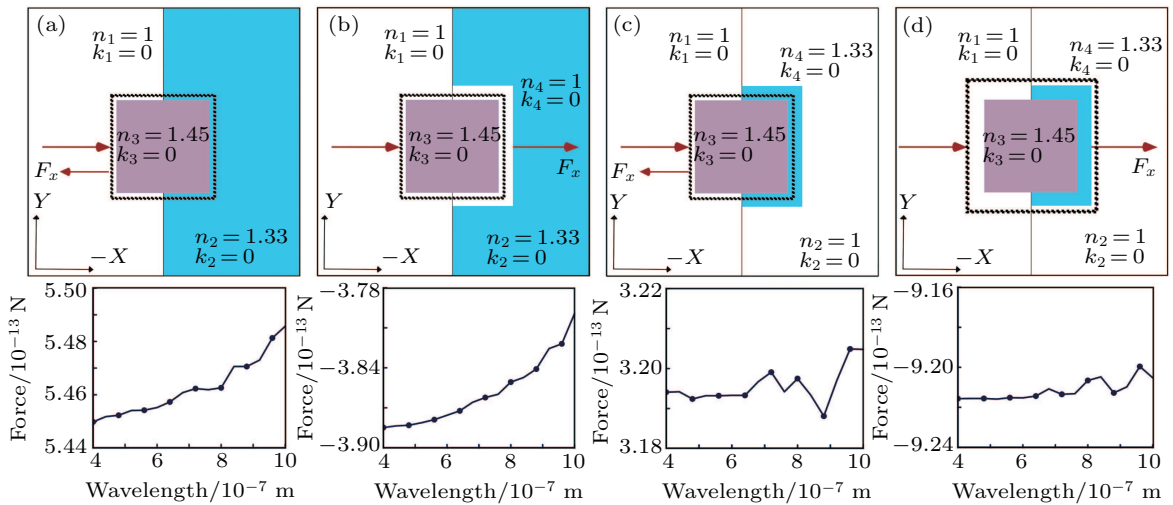

Fig. 5. Length of object at each side of the slab is 4000 nm and time averaged force has been calculated on silica using Eq. (1). The dash line represents the integration boundary. The light is propagating along $-x$ direction at different wavelength (range 400–1000 nm). The positive ($+$) force represents the pulling and the negative ($-$) force represents the pushing one. (a) Time averaged optical force is found pulling when long background is water for 2D, (b) pushing force when there is a small air gap between the object and the long background, (c) optical pulling force with short water background and long background air, and (d) optical pushing force when the integration boundary is just outside the short water background.

All these analytical (and full wave simulation based) observations are supporting the proposal that the interface of the two distinct media (and the entering and leaving momenta of photon at those interfaces) plays a vital role on the transfer of photon momentum. Notably, the linear increase of photon momentum [i.e., p_{Mink}] can be a consequence of reduced impedance mismatch at the interface of two distinct media as suggested in detail in Ref. [43].

3.3. Behavior of the transferred momentum of photon in the presence of absorption

Although for the non-absorbing object and non-absorbing background, the transferred momentum of photon usually increases, this scenario changes when applied in the presence of absorption, either in the sub-merged object or in the embedding lower background. At first, we can check the case of half immersed absorbing object. If we replace a half immersed non-absorbing dielectric by a lossy dielectric or a plasmonic object, it is clearly observed that the pulling force fully vanishes as shown in Figs. 6(a) (for 2D case) and 6(b) (for 3D case). The easiest possible experiment to verify this pushing force can be done by replacing the lossless silica object with a gold or a silver object in the well-known interfacial tractor beam experiment[12] and shining the usual Gaussian beam wave on it.[12] The findings and demonstrations in this article suggest that optical pushing force should be observed instead of optical pulling force in such a set-up. But the obvious question is this pushing force arising due to the transfer of Abraham momentum of photon to the half-immersed object or due to some other reason(s)? This issue is addressed in detail in the next part.
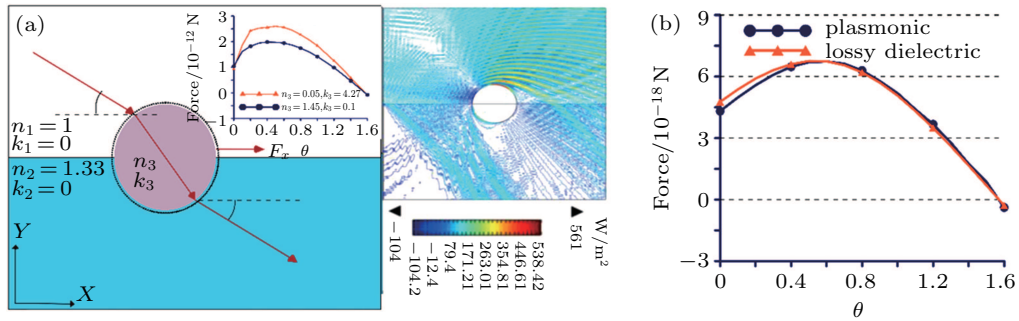

Fig. 6. Diameter of the object is 4000 nm and time averaged force on the object has been calculated using Eq. (1). The dash line represents the integration boundary. (a) The 2D cases. Right side inset: (i) an absorbing silica object (absorbing coefficient 0.1, lossy dielectric) or (ii) a plasmonic silver object half immersed in air and non-absorbing water. Inset: optical pushing force for different angles of incident light for both cases. Right side inset: Poynting vector (incident angle of 45° for plasmonic object (the absorbing silica case is also very similar, hence not shown here)). (b) 3D cases for both the objects with the same parameters of (a).

3.4. Explanation of the observed results for lossy objects

Now the first question is what actually happens in Fig. 6 (absorbing object half-immersed in lossless water). And the second question is what the possible differences between the non-absorbing situations and the absorbing cases are. Now, we shall investigate the idea both mathematically and intuitively as follows.

It is well known that Minkowski stress tensor[37–41,46–48] has a divergence free nature, which suggests that, if the Minkowski stress tensor is applied inside a non-absorbing object employing the internal field of the embedded object, it would lead to zero time-averaged total force. When absorption is introduced inside the half-immersed object, the force inside the absorbing object has a non-zero value equal to Eq. (2) [read Ref. [37] for more detail on Eq. (2)]. According to Refs. [37,42] that the same time averaged conduction force $\langle F_c^{in} \rangle$ in Eq. (2) (that arises due to the free currents inside the scatterer) can also be written by the volumetric force method[15,37,42]

$$\left\langle \boldsymbol{F}_{Mink.}^{Bulk} \right\rangle (in) = \left\langle \boldsymbol{F}_c^{in} \right\rangle = \int \langle f_c \rangle dv$$

$$= \int \frac{1}{2} \mathrm{Re}[(\omega \varepsilon_I \boldsymbol{E}_{in} \times \boldsymbol{B}_{in}^*) - (\omega \mu_I \boldsymbol{H}_{in} \times \boldsymbol{D}_{in}^*)] dv. \quad (18)$$

Here ε_I and μ_I are the imaginary parts of the permittivity and permeability of the scatterer, respectively. It should be noted that, if there is no absorption inside an object (i.e., lossless object), the total internal force $\left\langle F_c^{in} \right\rangle$ becomes zero which can be understood from Eq. (4) [as there would be no ε_I and μ_I in Eq. (4)].

The connection between previously discussed Eqs. (1) and (2) can be written as

$$\int \left\langle \overline{\overline{\boldsymbol{T}}}_{Mink.}(out) \right\rangle \cdot ds = \left\langle \boldsymbol{F}^{total} \right\rangle = \left\langle \boldsymbol{F}_{Mink.}^{Bulk} \right\rangle (in) + \left\langle \boldsymbol{F}_{Mink.}^{Surface} \right\rangle.$$

Previously discussed Helmholtz's force density gets an additional bulk part in the presence of loss and hence the total time averaged force density takes the form

$$\langle f_z \rangle = -(1/4)|\boldsymbol{E}|_x^2 (\partial \varepsilon_r / \partial z) \\ - [(1/2)\varepsilon_i \mathrm{Im}[\boldsymbol{E}_x(\partial \boldsymbol{E}_x^*/\partial z)]]. \quad (19)$$

According to the Minkowski's theory, there is no net force (bulk force) on the bound charges inside the lossless medium of the object/background.[37,42] For lossless

objects, all the forces are surface ones (stated above as Helmholtz force) occurring at the interface between the lossless object/background. But this is not the case for the lossy/absorbing cases according to our aforementioned discussion. Depending on the amount of loss (value of the absorption coefficient), the net force will turn from a pulling on to a pushing one as observed in our simulation results. For a lossy object, as the absorption coefficient increases from zero, the rate of momentum imparts on the free charges and hence momentum transfer via scattering on the material of the object increases and at a certain value, compensates the pulling force putting the object at equilibrium. After further increase of the absorption coefficient, the pushing force overcomes the pulling force and we get a net pushing force on the spherical

object (see our simulation results given in Fig. s2 of supplement material).

To illustrate these issues by using a simple mathematical analysis, let us consider an absorbing dielectric rectangular slab half embedded in a non-absorbing liquid dielectric medium. The pushing force has been verified by full wave simulation for a half-immersed slab in Figs. 7(a) (for lossy dielectric slab) and 7(b) (for plasmonic slab). According to the corpuscular theory, the time averaged force can be written like before

$$\langle \boldsymbol{F}_{\text{Total}}^{\text{Embedded}}(\text{out}) \rangle = \tau_{\text{i}} + \tau_{\text{r}} - \tau_{\text{t}} = N_{\text{i}} p_{\text{i}} + N_{\text{r}} p_{\text{r}} - N_{\text{t}} p_{\text{t}}. \quad (20)$$

Now, equation (20) can be written based on two fully different mathematical ways.
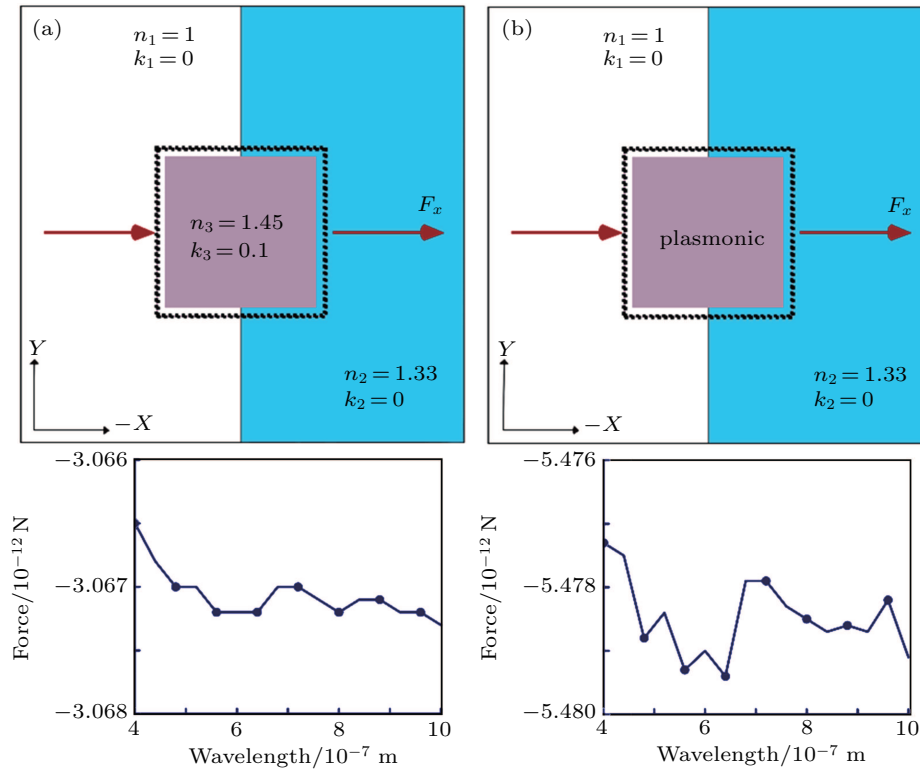

Fig. 7. Length of object at each side of the slab is 4000 nm and time averaged force has been calculated on the object using Eq. (1). The dahs line represents the integration boundary. The light is propagating along $-x$ direction at different wavelength (range 400–1000 nm). The positive (+) force represents the pulling and the negative (−) force represents the pushing one. Time averaged optical force on lossy object is found always pushing. (a) Optical pushing force occurs, when object is lossy dielectric, (b) pushing force occurs, when object is plasmonic.

(i) The first way is the straightforward one: by employing the Abraham momentum of photon in the transmitted medium (the lower touching background), which directly suggests that the pushing force occurs because of $N_{\text{i}} p_{\text{i}} + N_{\text{r}} p_{\text{r}} > N_{\text{t}} p_{\text{t}}$ (always),

$$\langle \boldsymbol{F}_{\text{Total}}^{\text{Embedded}}(\text{out}) \rangle = (1/2) |\boldsymbol{E}|_0^2 \varepsilon_0 [(1 + |R|^2) - (n_{\text{bt}})^{-1} |T|^2], \quad (21)$$

where n_{bt} is the refractive index of the lower touching background medium.

(ii) The second way is not the straightforward one: by

employing the Minkowski momentum of photon in the transmitted medium (the lower touching background), which does not directly suggest how the pushing force occurs following this equation:

$$\langle \boldsymbol{F}_{\text{Total}}^{\text{Embedded}}(\text{out}) \rangle = (1/2) |\boldsymbol{E}|_0^2 \varepsilon_0 [(1 + |R|^2) - (n_{\text{bt}}) |T|^2]. \quad (22)$$

Here,[50,51]

$$|T|^2 + |R|^2 = 1 - P_{\text{Loss}}. \quad (23)$$

If we put the value of $|T|^2$ in Eq. (22) from Eq. (23), we obtain

the equation

$$\left\langle \boldsymbol{F}_{\text{Total}}^{\text{Embedded}}(\text{out}) \right\rangle$$
$$= (1/2)|\boldsymbol{E}|_0^2 \varepsilon_0 [[(1-n_{\text{bt}})+|R|^2(1+n_{\text{bt}})]+n_{\text{bt}}P_{\text{Loss}}]. \quad (24)$$

Equation (24) suggests that if we consider the Minkowski momentum of photon in the transmitted medium, depending on the value of P_{Loss} (which is always found positive but changes with the absorption coefficient between 0 and 1 in Fig. 3(c) in Ref. [50]), the time averaged force can be pulling or pushing. According to Eq. (24), in presence of lower value loss, it can be possible to observe optical pulling force.

At the very first look, it appears that: process (i), which suggests in favor of Abraham momentum of photon, may have no trouble. But this conclusion leads to two notable problems: (1) the mathematical form along with the behavior of an equation of physics [i.e., Eq. (12) in this article] directly changes from one case [i.e., non absorbing situation] to another case [i.e., absorbing situation]. (2) According to Eq. (21), the optical pulling force should not occur even for the lower value of absorption [i.e., one can put Eq. (23) in Eq. (21) and easily verify it]. But our simulation results (shown in supplement s2) suggests that depending on the amount of loss (value of the absorption coefficient), the net force will turn from a pulling one to a pushing one gradually (but not abruptly). As a result, we conclude that when the object is lossy, a significant amount of the incident momentum will be transferred to the object due to absorption. Thus, the object overall gets a pushing force. However, the amount of momentum transferred (from the lower medium) is still the Minkwoski (as discussed in aforementioned process (ii)) but not the Abraham one by an abrupt switch. Depending on the amount of loss (value of the absorption coefficient), the net force will turn from a pulling one to a pushing one (as observed in our simulation results).

Hence, an obvious question arises: when the Abraham momentum of photon may appear. Is it a wrong momentum of photon? This issue is addressed in the next section.

3.5. The traveling momentum of photon in continuous background or host medium

According to Ref. [37], inside the absorbing dielectric slab, the conducting force of Eq. (18) takes the following form:

$$\langle f_{\text{c}} \rangle = (1/2)(n\omega/c)\varepsilon_{\text{i}}|\boldsymbol{E}|_x^2$$
$$= -(1/2)\,\text{Re}[(n/c)(\boldsymbol{\nabla} \cdot \boldsymbol{S})]. \quad (25)$$

According to Eq. (25), the transfer of momentum to free currents due to the attenuation of the wave in the medium is given by the divergence of the Minkowski momentum of photon in Eq. (25).[37] This dependence on refractive index (transfer of Minkowski momentum of photon) has also been observed in the dilute gas experiment[52] and photon drag measurement

for free charge carriers.[53] It suggests that the transferred momentum to the free charges inside any absorbing object can be considered as the one of Minkowski. Though the transferred momentum to the free carriers in the host semiconductor[4] is considered as the one of Minkowski, the traveling momentum of photon has been considered as the one of Abraham according to the detail analysis given in Ref. [4]: "It is clear that the experimental observations to date are consistent with both the Minkowski and Abraham momenta. The momentum transfer to a body (in our case the charge carriers) within a medium is given by the Minkowski momentum. The momentum of a photon travelling through a host dielectric, however, is given by the Abraham momentum. These results have both arisen from applying the same Lorentz force to a simple model dielectric, …"

However, for our proposed set-ups, the doubt arises for the lower continuous background medium. The reason is obvious: though the transferred momentum from this lower (touching) background to the half-immersed object is always the one of Minkowski (according to our previous detail discussions), does the Lorentz force analysis lead to the Abraham momentum of photon (traveling one) for the lower continuous background? This is analyzed next based on a simple thought experiment.

We have considered 2D set-ups given in Figs. 8(a) and 8(b): an object is half immersed in a long (but finite) background medium of water. The time averaged force on the lower continuous long (but finite) sized background can be calculated in two fully different ways: (I) by employing the external Minkowski stress tensor [cf. the integration boundary in Fig. 8(a)] and (II) by employing the Lorentz force method, applying the internal bulk force [cf. the integration boundary in Fig. 8(b)] and surface force method.[15,35,46,47] The total momentum conservation equation for the Lorentz volumetric force (whatever the form is chosen[54,55]) leads to the Abraham momentum of photon [cf. supplement s3 for detail analysis]

$$\nabla \cdot \overline{\overline{T_{\text{Lorentz}}}}(\text{inside a dielectric}) = \boldsymbol{f}_{\text{Lorentz}}(t) + \frac{\partial}{\partial t}\boldsymbol{G}(t), (26)$$

where $\overline{\overline{T_{\text{Lorentz}}}}$ is the associated stress tensor.[54] It is observed in Fig. 8(c) that the total time averaged forces calculated in two fully distinct ways are always in agreement with each other. The components [i.e., bulk and surface forces] of the total volumetric force are shown in Fig. 8(d). The detail calculation methods are given in supplement s3. This agreement between the external Minkowski force and internal Lorentz force (also commonly known as volumetric force) suggests that at least the instantaneous momentum of photon [i.e., the momentum density equation in Eq. (26)], which is traveling in the bulk part of the continuous lossless long background, can be modeled as the type of Abraham. This issue of Lorentz force distri-

bution inside water has been previously discussed in Ref. [54], which in all possible ways supports the Abraham[54] or field or kinetic[4,5] momentum of photon. For the lossless long background, if the Minkowski force is employed to yield the bulk force, it gives zero force due to the divergence free na-

ture of Minkowski stress tensor. As a result, probably there is no straightforward way to employ the Minkowski momentum of photon in the momentum conservation equation of Lorentz force (to yield the force on bulk medium inside lossless matter) stated above.
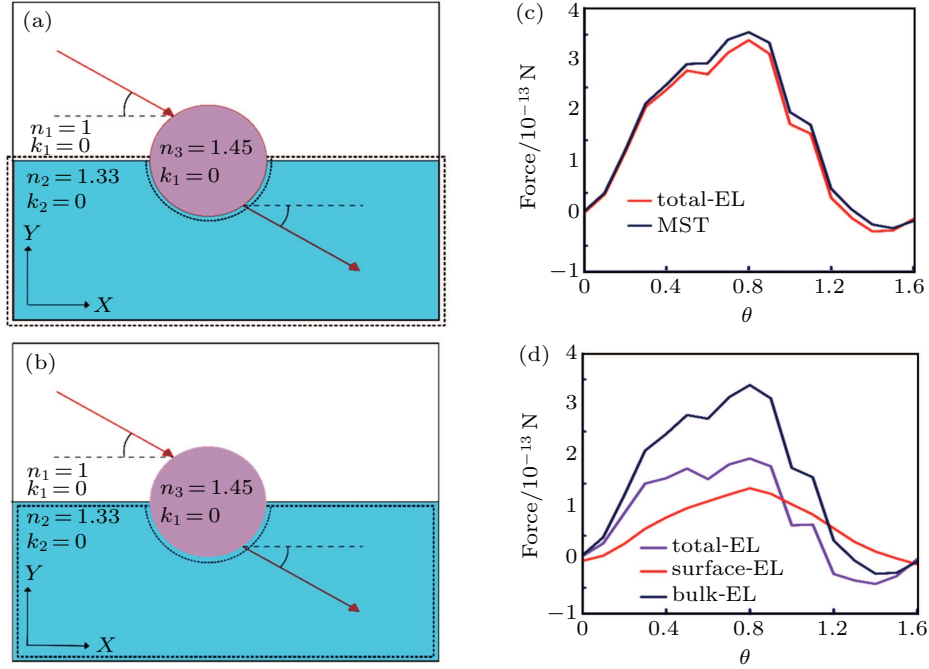

Fig. 8. Time averaged force (F_x) has been calculated on the long (but finite) water medium (not on the half-immersed object, which has diameter 500 nm) by using two different methods: time averaged external Minkowski stress tensor (MST) and Einstein–Laub (EL) force formulation (i.e., Lorentz volumetric force). To make the water medium much bigger than the half-immersed object, the vertical length of water medium is chosen 5000 nm and the horizontal length is 10000 nm. The dash line represents the integration boundary. (a) The outside optical force on long (but finite) water background is calculated by the integration of Minkowski stress tensor just outside the medium boundary (the dash line). (b) The dash line represents the integration boundary for calculating the internal bulk force on water medium using the EL force formulation and the surface-EL force is calculated just at the surface of the water medium. (c) Total time averaged optical forces (F_x) by external MST and volumetric EL force methods are in almost agreement. (d) Surface force, bulk force, and total optical force by using EL force formulation. It should be noted that the total force in EL force formulation is surface EL force + bulk EL force.

3.6. Application of machine learning techniques for predicting the type of optical forece

Finally, we take an interesting sidewalk from our primary focus and investigate whether machine learning based data analytics can provide us an accurate prediction on the time averaged optical force for the more generic cases based on the discussed complex set-ups in this article. The motivation behind this rather unusual investigation is as follows. A lot of parameters actually contribute towards determining the optical force type (i.e., pulling vs. pushing) and a full wave simulation[33,34] takes long time. In contrast, a quick accurate result in this regard could be extremely useful for experimental physicists at least to make quick primary decisions in many situations. So, we have made an attempt to develop a machine learning based system, using WEKA workbench,[56] which can accurately predict the outcome extremely faster. However, the accuracy of this prediction is naturally dependent on the dataset used for training the system. The dataset has been prepared based on some full wave simulations and is provided in chart 1s in the supplement material.

We have used the WEKA workbench[56] to develop the machine learning based classifiers and to conduct the computational experiments. The data given in the supplement s4 (chart 1s of the supplement) has been used to train a system that is able to predict the optical force type. In what follows, this data will be referred to as the training dataset. The varying parameters (i.e., features in the context of a machine learning model) used in the dataset are as follows: particle radius/lambda, particle loss, refractive index of the particle, background and short background, loss at long background and short background, and the short background width. Thus, chart 1s in the supplement material (supplement s4) has the first 8 columns for the parameters with the last (i.e., 9th) column representing the time averaged force experienced by the particle, here '1' ('0') represents optical pulling (pushing) force. The 9th column actually acts as the label for the training data. It should be noted that we have varied the incident angle of light from 0° to 90°, if the time averaged force is negative for most of the angles, we have defined it as 1, and in contrast, if the time averaged force is positive for most of the angles, we

have defined it as 0.

For our classification task, we have used a number of classifier algorithms, namely, Naïve Bayes,[57–59] simple logistics,[57,59,60] J48,[57,61] random forest,[57,62] random tree,[57,62] and so on. Following the machine learning literature, we have employed the 10-fold cross validation scheme: the training dataset is randomly partitioned into 10 equal sized subsets, of the 10 subsets, a single subset is retained as the validation data for testing the model, and the remaining 9 subsets are used as training data. The cross-validation process is then repeated 10 times, with each of the 10 subsets used exactly once as the validation data. The 10 results can then be averaged to produce a single estimation. Table 1 reports the accuracy measures found after performing 10-fold cross validation for each of the classifiers. From the results reported in Table 1, J48, random forest, and random tree classifiers have predicted the final results with the highest accuracy (more than 95%, which is quite satisfactory).

Table 1. The 10-fold cross validation results for different classifiers.

Sl.	Classifiers	Accuracy
1	Naïve Bayes	74.12%
2	simple logistic	83.07%
3	decision table	92.02%
4	Jrip	95.13%
5	J48	96.49%
6	random forest	97.27%
7	random tree	95.71%

So, given the values of the required parameters (i.e., features), our machine learning based predictor tool can be used to accurately and very quickly predict the force type. Apart from our motivation of getting a quick prediction of the force type without a time-consuming full wave simulation, this artificial intelligence-based investigation may open up a novel research avenue[63] by providing us with yet another useful tool/approach[63] to investigate other problems related to optical force[64] and photon momentum inside a matter.[65]

4. Conclusion

In this work, we have considered a distinct case — a particular configuration of light–matter interaction, i.e., an object (both non-absorbing and absorbing) is half immersed in an inhomogeneous or heterogeneous background, which can be very useful to conduct some very simple experiments to determine the transferred momentum of photon along with the traveling momentum of photon in a material medium. Considering our detail analysis in this work (and also several previous works), it appears that the transferred photon momentum to a half-immersed object (absorbing or non-absorbing) or a fully immersed/embedded object (or even to the free carriers inside an absorbing object) can better be modeled as the one

of Minkowski (where Minkowski momentum may arise exactly at the interface of two distinct media according to our analysis). But at the same time, we have demonstrated that though the transferred' momentum to a half-immersed Mie object (either lossy or lossless) can better be considered as the Minkowski momentum, optical Lorentz force analysis along with our full wave simulation results suggests that the momentum of a photon traveling through a host dielectric (i.e., in a continuous long background), however, can be considered as the type of Abraham momentum. Interestingly, this conclusion also supports the previous conclusion drawn in a notable work[4] for lossy semiconductor. Finally, based on several parameters, a machine learning based technique has been applied to quickly predict the time averaged total force, which may open up a novel research avenue by providing a useful tool/approach (i.e., artificial intelligence) to investigate other problems related to optical force and photon momentum inside a matter.

References

[1] Minkowski H 1908 Nachr. Ges. Wiss. Goettingen. Math. -Phys. Kl. 53–111. Reprint in 1910 Math. Ann. **68** 472
[2] Abraham M 1909 Rend. Cir. Mat. Palermo **28** 1
[3] Baxter C and Loudon R 2010 . Mod. Opt. **57** 830
[4] Barnett S M and Loudon R 2010 Phi. Trans. R. Soc. A **368** 927
[5] Barnett S M 2010 Phys. Rev. Lett. **104** 070401
[6] Zhang L, She W, Peng N and Leonhardt U 2015 New J. Phys. **17** 053035
[7] Kundu A, Rani R and Hazra K S 2017 Sci. Rep. **7** 42538
[8] She W, Yu J and Feng R 2008 Phys. Rev. Lett. **101** 243601
[9] Sukhov S and Dogariu A 2010 Opt. Lett. **35** 3847
[10] Chen J, Ng J, Lin Z and Chan C T 2011 Na. Photon. **5** 531
[11] Novitsky A, Qiu C W and Wang H 2011 Phys. Rev. Lett. **107** 203601
[12] Kajorndejnukul V, Ding W, Sukhov S, Qiu C W and Dogariu A 2013 Nat. Photon. **7** 787
[13] Brzobohaý O, Karásek V, Šiler M, Chvátal L, Čižmár T and Zemánek P 2013 Nat. Photon. **7** 123
[14] Qiu C W, Ding W, Mahdy M R C, Gao D, Zhang T, Cheong F C and Lim C T 2015 Light Sci. App. **4** e278
[15] Mahdy M R, Mehmood M Q, Ding W, Zhang T and Chen Z N 2017 Ann. Phys. **529** 1600213
[16] Zhu T, Novitsky A, Cao Y, Mahdy M R C, Wang L, Sun F and Ding W 2017 Appl. Phys. Lett. **111** 061105
[17] Brevik I 1979 Phys. Rep. **52** 133
[18] Brevik I 2018 Mo. Phys. Lett. A **33** 1830006
[19] Wang S, Ng J, Xiao M and Chan C T 2016 Sc. Adv. **2** e1501485
[20] Walker G B, Lahoz D G and Walker G 1975 Can. J. Phys. **53** 2577
[21] Partanen M, Häyrynen T, Oksanen J and Tulkki J 2017 Phys. Rev. A **95** 063850
[22] Partanen M and Tulkki J 2017 Phys. Rev. A **96** 063834
[23] Hinds E A and Barnett S M 2009 Phys. Rev. Lett. **102** 050403
[24] Leonhardt U 2014 Phys. Rev. A **90** 033801
[25] Kemp B A 2011 J. Appl. Phys. **109** 111101
[26] Pfeifer R, Nieminen T, Heckenberg N R and Rubinsztei-Dunlop H 2007 Rev. Mod. Phys. **79** 1197
[27] McDonald K T 2015 Bibliography on the Abraha-Minkowski Debate
[28] Brevik I 2018 Phys. Rev. A **98** 043847
[29] Wang C 2018 Optik **172** 1211
[30] Kemp B A and Grzegorczyk T M 2011 Opt. Lett. **36** 49
[31] Mansuripur M 2009 Phys. Rev. Lett. **103** 019301
[32] Brevik I 2009 Phys. Rev. Lett. **103** 219301
[33] Comsol A B 2007 COMSOL Multiphysics reference manual, Version 5.3
[34] Lumerical FDTD 2013 Solutions, Inc. A commercia-grade simulator based on the finit-difference tim-domain method was used to perform the calculations, Vancouver, Canada

[35] Mahdy M R, Zhang T, Danesh M and Ding W 2017 *Sc. Rep.* **7** 693
[36] Zhu T, Mahdy M R C, Cao Y, Lv H, Sun F, Jiang Z and Ding W 2016 *Opt. Express* **24** 18436
[37] Kemp B A, Grzegorczyk T M and Kong J A 2006 *Phys. Rev. Lett.* **97** 133902
[38] Zhang T, Mahdy M R C, Liu Y, Teng J, Lim C T, Wang Z and Qiu C W 2017 *ACS Nano* **11** 4292
[39] Gao D, Ding W, Nieto-Vesperinas M, Ding X, Rahman M, Zhang T and Qiu C W 2017 *Light Sc. Appl.* **6** e17039
[40] Niet-Vesperinas M, Sáenz J, Góme-Medina R and Chantada L 2010 *Opt. Express* **18** 11428
[41] Milonni P W and Boyd R W 2010 *Adv. Opt. Photon.* **2** 519
[42] Rahaman M H and Kemp B A 2017 *APL Photon.* **2** 101301
[43] Mansuripur M and Zakharian A R 2010 *Opt. Commun.* **283** 355
[44] Laskar J M, Kumar P S, Herminghaus S, Daniels K E and Schöter M 2016 *Appl. Opt.* **55** 3165
[45] Frias W and Smolyakov A I 2012 *Phys. Rev. E* **85** 046606
[46] Rivy H M, Mahdy M R C, Jony Z, Masud N, Satter S S and Jani R 2019 *Opt. Commun.* **430** 51
[47] Satter S S, Mahdy M R C, Ohi M A R, Islam F and Rivy H M 2018 *J. Phys. Chem. C* **122** 20923
[48] Mahdy M R, Danesh, Zhang T, Ding W, Rivy H, Chowdhury A B and Mehmood M Q 2018 *Sci. Rep.* **8** 316
[49] Kemp B A, Grzegorczyk T M and Kong J A 2005 *Opt. Express* **13** 9280
[50] Sabah C 2008 *Acta Phys. Pol. A* **113** 1589
[51] Sabah C, Tugrul Tastan H, Dincer F, Delihacioglu K, Karaaslan M and Unal E 2013 *Pro. Electromagn. Res.* **138** 293
[52] Campbell G K, Leanhardt A E, Mun J, Boyd M, Streed E W, Ketterle W and Pritchard D E 2005 *Phys. Rev. Lett.* **94** 170403
[53] Gibson A F, Kimmitt M F and Walker A C 1970 *Appl. Phys. Lett.* **17** 75
[54] Mansuripur M, Zakharian A R and Wright E M 2013 *Phys. Rev. A* **88** 023826
[55] Mansuripur M, Zakharian A R and Moloney 2006 *Proc. SPIE Conf.* **6326** 63260
[56] Witten I H, Frank E, Hall M A and Pal C J 2016 *Morgan Kaufmann*
[57] Tan P N 2005 *Introduction to data mining* (Pearson Education India)
[58] Reddy S, Kodali S R and Gundabathina J L 2012 *Int. J. Comput. Appl.* **58** 7
[59] Farid D, Zhang L, Rahman C, Hossain M A and Strachan R 2014 *Expert Syst. Appl.* **41** 1937
[60] Khalajzadeh H, Mansouri M and Teshnehlab M 2014 *Soft Computing in Industrial Applications. Advances in Intelligent Systems and Computing* 223 (Cham: Springer)
[61] Patil T R and Sherekar S S 2013 *Int. J. Compu. Sci. Appl.* **6** 256
[62] Kalmegh S R 2015 *Int. J. Emerging Techno. Adv. Eng.* **5** 507
[63] Xu Y 2018 *Chin. Phys. B* **27** 118901
[64] Ge C X, Wu Z, Bai J and Gong L 2019 *Chin. Phys. B* **28** 024203
[65] Brevik I 2017 *Ann. Phys.* **377** 1